Article

31P NMR Investigations on Roundup Degradation by AOP Procedures

Marcin H. Kudzin [1,*]**, Renata Żyłła** [1] **, Zdzisława Mrozińska** [1] **and Paweł Urbaniak** [2]

[1] Textile Research Institute, Brzezinska 5/15, Lodz 92-103, Poland; zylla@iw.lodz.pl (R.Ż.); zmrozinska@iw.lodz.pl (Z.M.)

[2] Faculty of Chemistry, University of Lodz, Tamka 12, Lodz 90-136, Poland; pawelurb@chemia.uni.lodz.pl

* Correspondence: kudzin@iw.lodz.pl; Tel.: +48-42-6163-100

Abstract: The reactions of (*N*-(PhosphonoMethyl)Glycine) PMG with H_2O_2 in homogenous systems were investigated using 31P NMR (Nuclear Magnetic Resonance). These reactions were carried out in two reaction modes: without UV radiation and under UV radiation. The reactions of PMG with H_2O_2 without UV radiation were carried out in two modes: the degradations of PMG (0.1 mmol) by means of 5–10 molar excess of hydrogen dioxide (PMG-H_2O_2 = 1:5 and 1:10) and the degradation of PMG (0.1 mmol) in homogenous Fenton reactions (PMG-H_2O_2-Fe^{2+} = 1:10:0.05 and 1:10:0.1). All reactions were carried out at ambient temperature, at pH 3.5, for 48 h. The reactions of PMG (in Roundup herbicide composition, 12 mmol) with H_2O_2 under UV radiation (254 nm) were carried out using $5 \times$ molar excess of H_2O_2 (60 mmol), in the pH range of $2 \leq pH \leq 12$, for 6 h. In this mode of PMG oxidation, the splitting of C-P was observed in the ratios dependent on the applied pH of the reaction mixture.

1. Introduction

Glyphosate (*N*-(PhosphonoMethyl)Glycine) (PMG) is a broad-spectrum systemic herbicide, invented by Franz and brought to market in 1974 by Monsanto under the trade name Roundup [1,2].
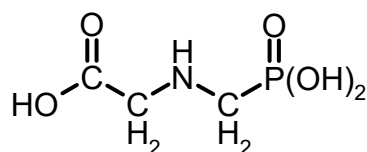
PMG

Glyphosate, absorbed mainly through foliage, inhibits a plant enzyme—5-enolpyruvylshikimate-3-phosphate (EPSP) synthetase (EC 2.5.1.19)—involved in the bio-synthesis of aromatic amino acids (AAA) substrates in a build-up of plant lignins [3–5].

A significant fraction of glyphosate sprayed on crops returns to the soil, and in spite of strong adsorption to soil solids [6], is able to contaminate surface water (runoff and erosion) [7–9].

Animal and epidemiological studies published in recent decades point to a potential glyphosate toxicity [10–12]. Further, the World Health Organization's International Agency for Research on Cancer concluded that glyphosate is "probably carcinogenic to humans" [13] and Anifandis et al. [14,15] demonstrated that glyphosate/PMG induce DNA fragmentation.

Therefore, various treatment processes have been investigated to reduce the pesticide concentration in water and to minimize the potential health risks associated with exposure to these

chemicals by the consumption of contaminated water [16–26]. Advanced oxidation processes (AOPs) are a key technology to solve pesticide contamination problems during both water and wastewater treatment (Table 1).

Table 1. Representative applications of advanced oxidation process (AOP) technology in the chemical degradation of *N*-(PhosphonoMethyl)Glycine (PMG) and aminomethylphosphonic acid (Gly^P).

No	P-Herbicide	AOP Systems	Phosphorus Degradation Products	Analysis	Reference
1	PMG and Gly^P	Birnessite (Mn^{4+} and Mn^{3+})	H_3PO_4	VIS (P-Mo Blue)	[20]
2	PMG	Fe$^{(III)}$(C$_2$O$_4$)$_n$$^{m-}$/UV (365 nm)	H_3PO_4	VIS (P-Mo Blue)	[21]
3	PMG	TiO$_2$/UV (312 nm)	H_3PO_4	HPLC-UV	[22]
4	PMG	O$_2$/TiO$_2$/SiO$_2$/UV (365 nm)	H_3PO_4	TOC, HPLC	[23]
5	PMG and Gly^P	O$_3$ (pH = 6.5 and 10) Photolysis (292 nm) TiO$_2$/O$_2$ (292 nm)	H_3PO_4 H_3PO_4 H_3PO_4	TOC, HPLC-FD TOC, HPLC-FD TOC, HPLC-FD	[24]
6	PMG	H$_2$O$_2$/UV (254 nm)	H_3PO_4	HPLC-FD	[25]
7	PMG	Birnessite (Mn^{4+} and Mn^{3+})	H_3PO_4 + Gly^P + C-P^x	^{31}P NMR	[26]

Birnessite (Na$_{0.3}$Ca$_{0.1}$K$_{0.1}$)(Mn^{4+}, Mn^{3+})$_2$O$_4$ × 1.5 H$_2$O. Fe$^{(III)}$(C$_2$O$_4$)$_n$$^{m-}$ – Fe(C$_2$O$_4$)$_2$$^-$ and Fe(C$_2$O$_4$)$_3$$^{3-}$. P$_i$ colorimetrical determination using the phospho-molybdate blue reaction. TOC—total carbon. C-P^x—unidentified compound.

The various mechanisms of PMG degradation using AOP technology, according to the literature, were presented by Manassero [25]. These not always coherent results (Figure 1) led us to investigate these process by using ^{31}P NMR monitoring of the PMG degradation processes. This ^{31}P NMR technique has been applied for the analysis of PMG metabolites and degradation products in only a few earlier research works [26–33].
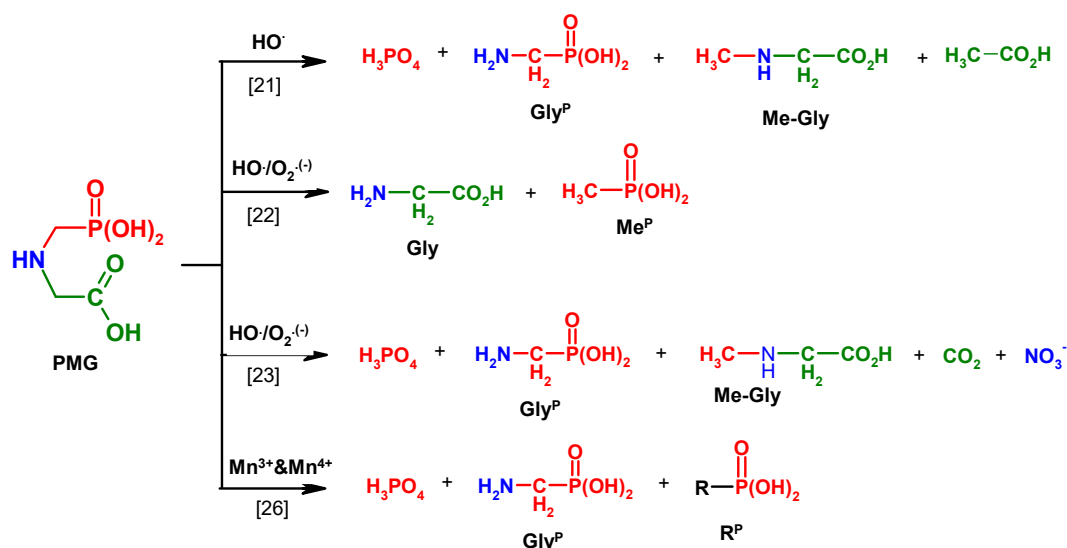

Figure 1. Degradation products of *N*-PhosphonoMethyl)Glycine (PMG) of representative methods.

2. Materials and Methods

2.1. Materials

The phosphonic amino acids used in the studies (Table 2) were synthesized as follows: aminomethylphosphonic acid (Gly^P) was synthesized according to the Soroka method [34,35]; (*N*-methylamino)methylphosphonic acid (Me-Gly^P) was obtained by the hydrophosphonylation of 1,3,5-trimethylhexahydro-1,3,5-triazine by means of diisopropylphosphite according to

Maier [36]; (*N,N*-dimethylamino)-methyl-phosphonic acid (Me$_2$-Gly^P) was obtained by the modified Kabachnik-Fields condensation [37,38].

Table 2. Names, abbreviations, and structures of aminophosphonic acids discussed in this work [a].

Structure			Name	Trivial Name	Abbr.	
$\begin{array}{c} R^1 \\ \diagdown \quad\quad O \\ \quad\quad \| \\ N-C-P(OH)_2 \\ R^{2\diagup} \quad H_2 \end{array}$			1-aminoalkylphosphonic acid	phosphono amino acid	AA^P	Synth.
No	R	R^1				
1	H	H	aminomethylphosphonic acid	phosphono-glycine	Gly^P	[35]
	Me	H	(*N*-methylamino)methyl-phosphonic acid	phosphono-(*N*-methyl)-glycine	Me-Gly^P	[37]
	Me	Me	(*N,N*-dimethylamino)-methylphosphonic acid	phosphono-(*N,N*-dimethyl)-glycine	Me$_2$-Gly^P	

[a] Applied names are in accordance with the IUPAC rules, and abbreviations are in agreement with the general rules elaborated by [38,39].

Phosphonomethyl glycine, methylphosphonic acid, 1,3,5-trimethylhexahydro-1,3,5-triazine, catalase and other applied reagents and solvents were purchased from Aldrich. Diisopropylphosphite was purchased from ACROS Organic^{TM}.

Herbicide Roundup Ultra 170 SL, containing glyphosate-isopropylammonium salt [227.2] (CAS: 38641-94-0; 170 g/L; 15.67%; 0.75 M), and surfactant (CAS not given; 8%) were purchased from Monsanto Europe S.A (Scotts Poland, Warsaw, Poland).

2.2. Synthesis of Aminophosphonic Standards

2.2.1. Synthesis of Aminomethylphosphopnic Acid (Gly^P)

Phosphorus chloride(III) (8.75 mL; 0.10 mol) was added dropwise to a well-stirred mixture of *N*-(hydroxymethyl)benzamide (synthesized by the hydroxymethylation of benzamide [34]) (15.1 g; 0.10 mol) and anhydrous acetic acid (20 mL), at ambient temperature. The mixture was then refluxed for 1 h, evaporated (25 °C at 10–20 mm Hg for 15 min, and 75 °C at 0.05 mm Hg) to an oily residue and dissolved in hydrochloric acid solution (5 M aq.; 100 mL). The mixture was heated under reflux for 8 h, cooled to room temperature, and the separated benzoic acid was filtered off. The filtrate was evaporated, the residue was dissolved in water (20 mL), then the solution of crude Gly^P was purified on a Dowex 50 W × 8 ion exchange column using water elution. The obtained Gly^P (8.1 g; 0.072 mol; 72%) was homogeneous at ^{31}P NMR solutions. Elemental analysis data (determined %/(calculated %)) for CH$_6$NPO$_3$ [111.04] C = 10.70 (10.82); H = 5.47 (5.45); N = 12.50 (12.61).

2.2.2. Synthesis of *N*-Methylaminomethylphosphopnic Acid (Me-Gly^P)

To trimethylhexahydro-s-triazine (1.29 g; 0.01 mol diisopropylphosphite (5.0 g; 0.03 mol), was added and the mixture was heated with stirring to 100–110 °C for 4 h. The reaction mixture was evaporated (25 °C at 10–20 mm Hg for 15 min, and 75 °C at 0.05 mm Hg), then diluted with 5 M HCl (100 mL) and refluxed for 8 h. The hydrolyzate was evaporated to an oily residue, which was dissolved in water (20 mL) and extracted with ethyl ether (20 mL). The aqueous layer was passed through a Dowex 50 W × 8 ion exchange column using water elution. Fractions were collected (molybdate test) and evaporated. The crystalline product was washed with ethanol, filtered, and dried to give 2.0 g (53.3%) of Me-Gly^P, homogeneous ^{31}P NMR solutions. Elemental analysis data (determined %/(calculated %)) for C$_2$H$_8$NPO$_3$ [125.06]: C = 19.12 (19.21); H = 6.55 (6.45); N = 11.10 (11.2).

2.2.3. Synthesis of *N,N*-Dimethylaminomethylphosphopnic Acid (Me$_2$-Gly^P)

The formaldehyde aqueous solution (37%; d = 1.11 g/mL; 2.9 g; 0.05 mol) was gradually added to a stirred mixture of equimolar quantities of dimethylamine (2 M solution of Me$_2$NH in methanol; 25 mL; 0.05 mol) and diethyl phosphite (7.8 g; 0.05 mol), keeping the temperature below 85 °C. The reaction mixture was stirred for 30 min, and evaporated (25 °C at 10–20 mm Hg for 15 min, and 75 °C at 0.05 mm Hg) to an oily residue. The residue was dissolved in 5 M HCl (100 mL) and the solution was refluxed for 8 h. The hydrolyzate was evaporated to dryness (60 °C; 10–20 mm), and the residue was passed through a Dowex 50 W × 8 ion exchange column using water elution. The collected fractions (phosphomolybdate assay) were evaporated to dryness giving white crystals of Me$_2$Gly^P (4.2 g; 60.0%), homogeneous in^{31}P NMR solutions. Elemental analysis data (determined %/(calculated %)) for C$_3$H$_{10}$NPO$_3$ [139.09]: C = 25.78 (25.91); H = 7.32 (7.25); N = 9.98 (10.07).

2.2.4. Solutions

- Solution of 0.01 M Fe(II): a sample of FeSO$_4$ × 7H$_2$O [278] (28 mg) was dissolved in water (10 mL).
- Solution of 0.02 M Fe(II): a sample of FeSO$_4$ × 7H$_2$O [278] (56 mg) was dissolved in water (10 mL).
- Catalase solution: a sample of 10 mg of catalase was dissolved in 50 mL of distilled or deionized water.
- Solution of 2 M H$_2$SO$_4$ (in 20% D$_2$O): samples of 2.5 M H$_2$SO$_4$ (20 mL) were diluted to 25 ml with D$_2$O (5 mL).

2.3. Instruments

^{31}P NMR spectra were recorded on a Bruker AC 200 spectrometer operating at 81.01 MHz and on a Bruker Avance III 600 spectrometer operating at 242.9 MHz. ^{1}H NMR spectra were recorded on a Bruker Avance III 600 spectrometer operating at 600 Hz. Positive chemical shift values of ^{31}P were reported for compounds absorbed at lower fields than H$_3$PO$_4$.

The pH measurements were performed using a CX-505 multifunction laboratory meter (Elmetron, Zabrze, Poland) equipped with a combination pH electrode EPP-1 (Elmetron, Zabrze, Poland). The chemical degradation of aqueous solutions of the Roundup herbicide formulation in PMG-H$_2$O$_2$ and PMG-H$_2$O$_2$-UV systems was carried out. Experiments were performed in the reactor shown in Figure 2.
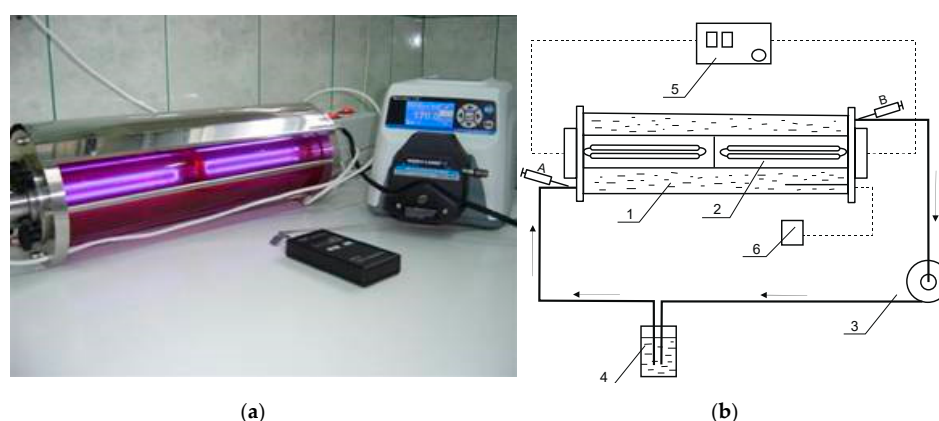

(**a**) (**b**)

Figure 2. Reactor used for Roundup degradation by means of AOP technology. (**a**) Figure of a photoreactor with UV lamp used for the oxidation of PMG by means of UV/H$_2$O$_2$. (**b**) Schematic diagram: 1—glass reactor; 2—quartz tube with UV lamp (254 nm; 22 W); 3—peristaltic pump; 4—reactor connector; 5—UV power supply; 6—temperature detector; A, B—samples. Applied conditions: PMG (12 mmol), H$_2$O$_2$ (60 mol) in an aq. solution (3.7 L) at different initial pH values applied: 2 ≤ pHs ≤ 12. Irradiation time was up to 360 min. Temperature was 25 °C.

2.4. Degradation of Glyphosate

2.4.1. Degradation of Phosphonomethyl Glycine (PMG)

Samples of PMG (0.1 mmol) were dissolved in appropriate volumes of $FeSO_4$ solution (0.5 mL of 0.01 M/0.02 M solution of $FeSO_4$), followed by the addition of dihydrogen dioxide (the exact amounts of the solutions are given in Table 3) and kept at room temperature for a desired reaction time. Then, the reaction mixtures were centrifuged, acidified with 2 M H_2SO_4 to pH = 3.5 if necessary, and the volumes of 0.4 mL were taken and mixed with D_2O (0.05 mL) and 0.1 M EDTA (0.05 mL), and analyzed by means of ^{31}P NMR.

Table 3. Preparation of the reaction mixtures for $PMG-H_2O_2$ and $PMG-H_2O_2-Fe^{2+}$ systems.

Exp.	PMG 0.1 mmol	H_2O	10 M H_2O_2		$FeSO_4$	
			0.5 mmol	1 mmol	0.01 M	0.02 M
1	17 mg	0.55 mL	0.05 mL	–	–	–
2	17 mg	0.5 mL	–	0.1 mL	–	–
3	17 mg	–	–	0.1 mL	0.5 mL (0.005 mmol)	–
4	17 mg	–	–	0.1 mL	–	0.5 mL (0.01 mmol)

2.4.2. Degradation of Roundup Herbicide Formulation by Means of AOP Technology

Reaction mixtures were prepared in accordance with Table 4. Thus, samples of PMG contained in Roundup Ultra 170 SL Herbicide solution (0.75 M; 16 mL; 12 mmol of PMG), were diluted in water (3680 mL), dihydrogen dioxide samples (60 mmol) were added, and the reaction mixtures were adjusted to the desired pH value by means of acidification with 2 M H_2SO_4 or alkalized by means of 5 M KOH. The oxidative degradations of herbicide were performed for the desired time, during which the reaction progress was monitored by the ^{31}P NMR analysis. Thus, the appropriate samples (4 mL) were treated with catalase (0.1 mL), kept for 30 min at room temperature, and evaporated to an oily residue. These were dissolved in 2 M H_2SO_4 (in 20% D_2O) (0.5 mL) and analyzed using ^{31}P NMR.

Table 4. Preparation of the reaction mixtures for AOP degradations of PMG in Roundup herbicide.

No	Roundup (0.75 M)		H_2O	H_2O_2 (30%; 10 M)		H_2SO_4 (2 M)	NaOH (5 M)	pH
	mL	PMG mmoL	mL	mL	mmoL	mL	mL	
1	16.0	12.0	3 680	–	–	–	–	4.85
2	16.0	12.0	3 680	6.0	60.0	4.6	–	2.0
3	16.0	12.0	3 680	6.0	60.0	0.5	–	4.0
4	16.0	12.0	3 680	6.0	60.0	–	4.0	6.0
5	16.0	12.0	3 680	6.0	60.0	–	4.8	8.0
6	16.0	12.0	3 680	6.0	60.0	–	6.0	10.0
7	16.0	12.0	3 680	6.0	60.0	–	40.0	12.0

3. Results and Discussion

3.1. Protonation Equilibria of Reagents

Representative values of pK_a are given in Table 5. On this basis, protonation equilibria of phosphonomethyl glycine (PMG) are presented in Figure 3.

Table 5. Representative works on pKa determination of PMG.

| No. | pK | | | | Method | Reference |
	pK_1	pK_2	pK_3	pK_4		
1	2.0	2.6	5.6	10.6	pH metric titration	[40]
2		2.32	5.86	10.86	pH metric titration	[41]
3	<1	2.0	5.5	10.5	^{1}H and ^{31}P NMR	[42]
4	0.3	2.3	5.6	10.6	^{1}H and ^{31}P NMR	[43]
5		2.09	5.52	10.28	pH metric titration	[44]
6		logβ 9.66 (1.58)	logβ 14.86 (5.20)	log β 16.44 (9.66)	pH metric titration	[45]
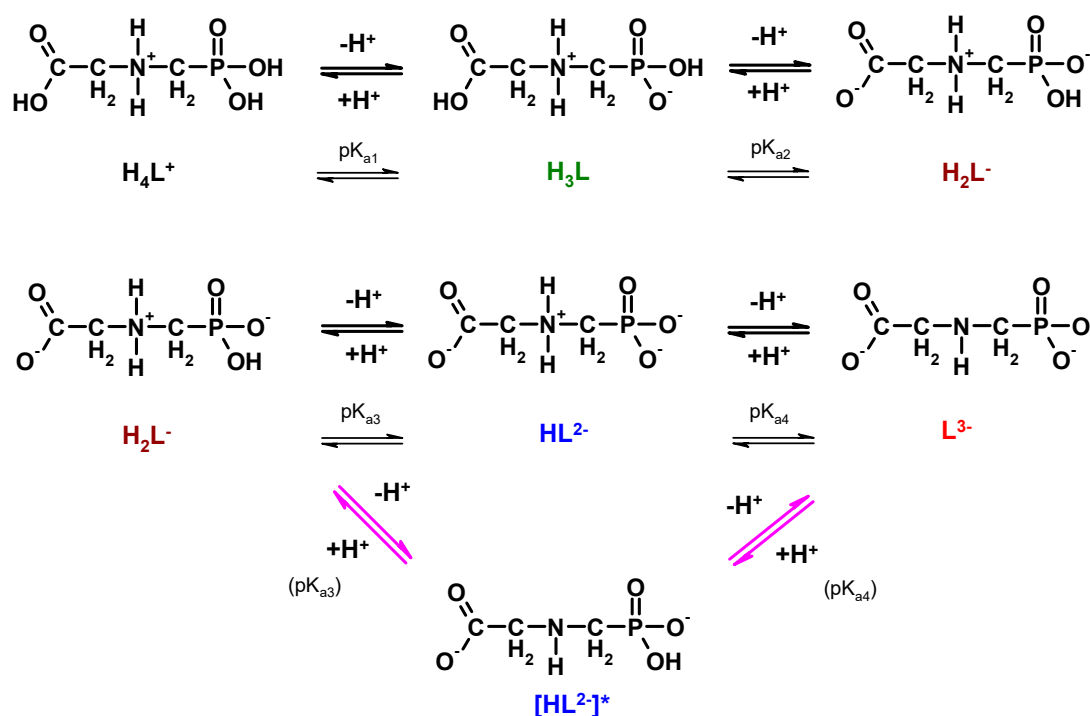
Figure 3. Dissociation/protonation equilibria of glyphosate (lower branch (arrows in magenta) considering the reports of Peixoto et al., 2015 [45] and Liu et al., 2016 [46]).

Despite the large amount of research data, there is conflicting information in the literature concerning the first protonation step of glyphosate, namely whether the first dissociable proton in the HL^{2-} formations is attached to the nitrogen atom of the amino group or to the oxide atom of the phosphonate function. As a matter of fact, only two recent reports consider that the first protonation step occurs on the one of the oxygen atoms in the phosphonate group (Figure 4, magenta arrows) [45,46].

On the basis of this analysis of the speciation graph (Figure 4), we assumed that in aqueous solutions PMG exists in the following forms: at pH = 0—mainly as H$_4$L$^+$ form; at pH = 1.5—mainly as H$_3$L form; at pH = 3.5–4—mainly as H$_2$L$^-$; at pH = 8—mainly as HL^{2-}; and at pH ≥ 12—mainly as L^{3-} form.
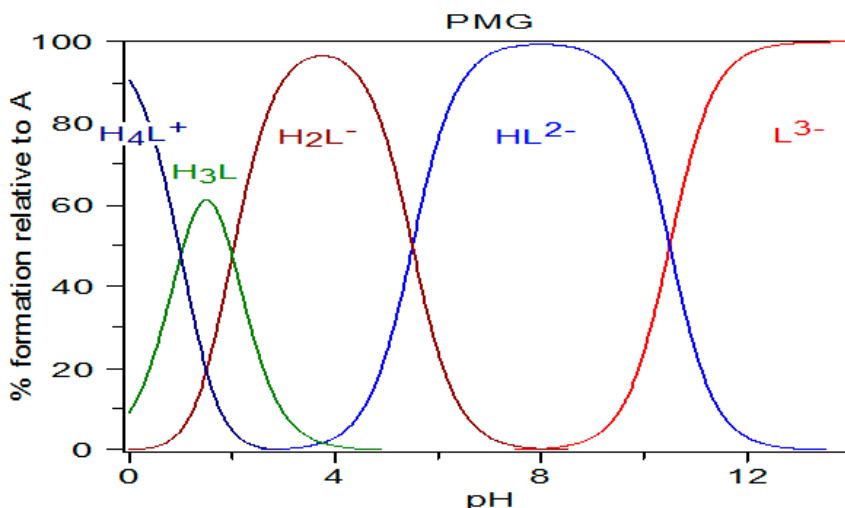
Figure 4. Diagram of PMG species distribution calculated using the pK_a values of Appleton et al. [42] ($pK_{a1} < 1$; $pK_{a2} = 2.0$; $pK_{a3} = 5.5$; $pK_{a4} = 10.5$), and the HySS program (Alderighi et al., 1999) [47].

The protonation equilibrium of dihydrogen dioxide is shown in Figure 5; dihydrogen dioxide speciation is also presented in Figure 6. In the literature, the pKa values for H_2O_2 are as follows: $pK_{a1} = -3.1$ [48] and $pK_{a2} = 11.6$ [49]. This means that in concentrated H_2SO_4 (e.g., 2 M), dihydrogen dioxide can exist in the H_3L^+ form, at pH = 0–8 it exists in the molecular form H_2L, at pH = 14 it is dissociated in ca. 50% to HL^-, and for 2 M KOH (pH > 14) it is almost fully ionized.
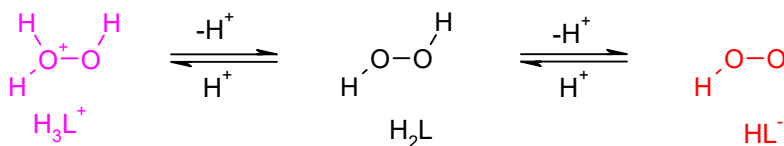
Figure 5. Dissociation/protonation equilibria of dihydrogen dioxide.
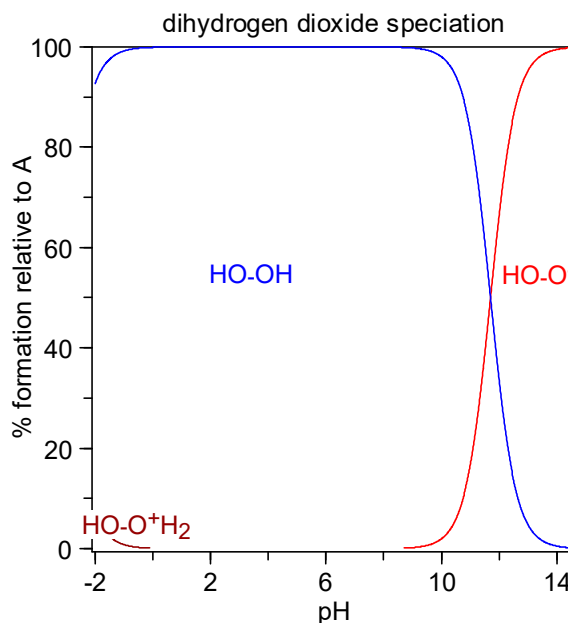
Figure 6. Diagram of dihydrogen dioxide distribution: percent species formation calculated with the HySS program (Alderighi et al., 1999) [47] for a 10 millimolar solution of H_2O_2 ($pK_{a1} = -3.1$, $pK_{a2} = 11.7$).

3.2. Reaction of PMG and H_2O_2

It is generally known that the oxidation potential of H_2O_2 greatly increases during UV irradiation (Mierzwa et al., 2018, and references cited therein) [50] as well as in the presence of metal ions (Figure 7) [50–55].
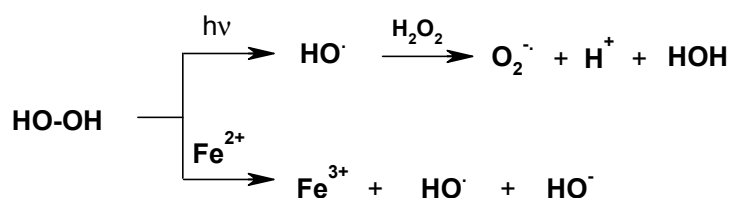

Figure 7. Activation of dihydrogen peroxide via the generation of radicals.

Therefore, we assumed that the reaction between PMG and dihydrogen peroxide consumed either the molecular form of H_2O_2 in the absence of irradiation, or hydroxide and peroxide radicals during UV irradiation or in the presence of Fenton reagents. The results of PMG degradation in both modes are illustrated in Figure 8.
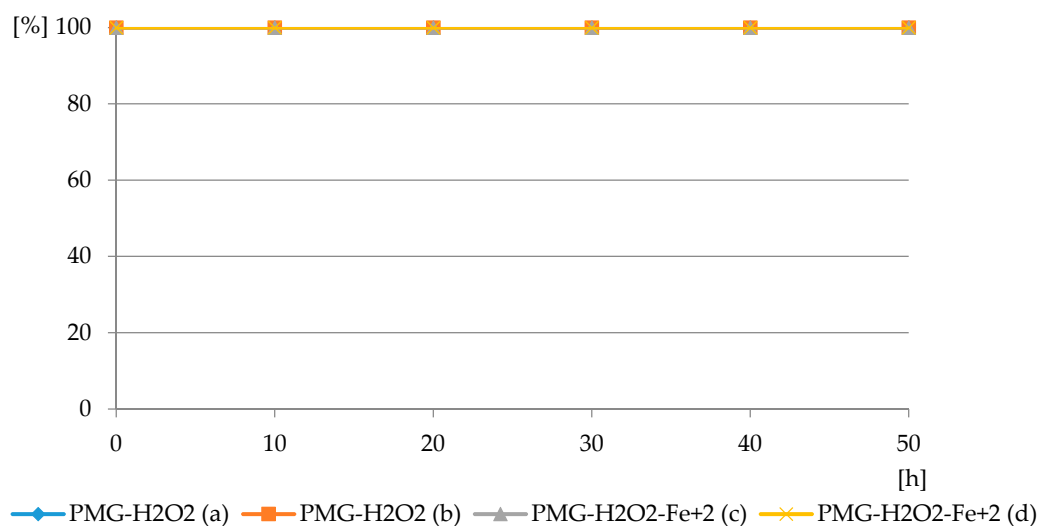
Figure 8. The profiles of PMG consumption in reaction with H_2O_2 in PMG-H_2O_2 and PMG- H_2O_2-Fe^{2+} systems at pH = 3.5: PMG:H_2O_2 = 1:5 (PMG-H_2O_2 (a)) and 1:10 (PMG-H_2O_2 (b)); PMG:H_2O_2:Fe^{2+} = 1:10:0.05 (PMG-H_2O_2-Fe^{2+} (c)); and 1:10:0.1 (PMG-H_2O_2-Fe^{2+} (d)) (residual PMG (%) vs. exposure time (h)).

The reaction of PMG with H_2O_2, both with H_2O_2 and H_2O_2-Fe^{3+}, did not occur at the applied pH = 3.5, at which PMG exists mainly in the H_2L^- protonated on nitrogen form (Figures 3 and 4) and hydrogen peroxide mainly in H_2L forms (Figures 5 and 6). Therefore, we assumed that the protonation of the amino function in PMG efficiently reduces the interaction of PMG and H_2O_2 (no trace of P-C bond splitting was observed in a 48-h period) (Figure 8). However, during the irradiation of aqueous solutions of PMG (in the form of the herbicide Roundup) and H_2O_2 (1:5), for a pH range of $2 \leq$ pH ≤ 12, the splitting of the P-C bond of PMG was observed, to an extent dependent on the pH of the applied solution (Figures 9 and 10). Is worth noting that the irradiation of aqueous PMG solution without H_2O_2 during a 48-h period did not exhibit any sign of PMG decomposition (100% of PMG).
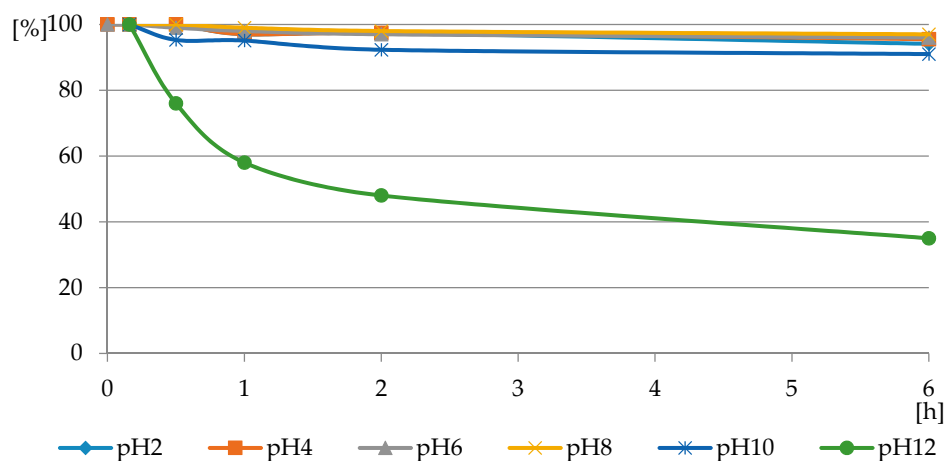
Figure 9. The profile of PMG consumption in reactions with H_2O_2 in PMG-H_2O_2-(UV) systems (with UV irradiation) carried out at a pH range of $2 \leq pH \leq 12$ and a temperature of 25 °C (residual PMG (%) vs. exposure time (h)).
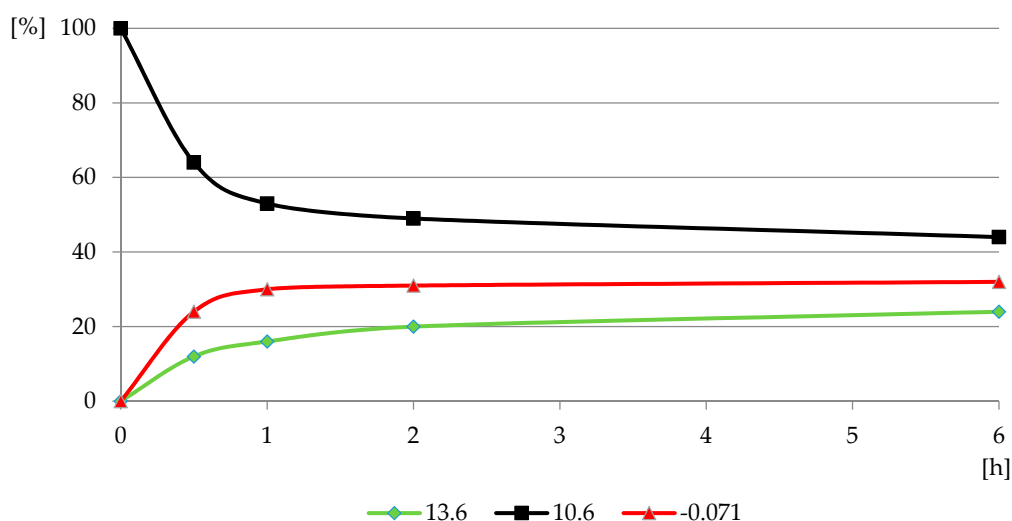

Figure 10. The profile of PMG reaction with H_2O_2 in PMG-H_2O_2-(UV) systems (UV; 25 °C) carried out at pH = 12 (relative P-compounds contribution (Gly^P: 13.6 ppm, PMG: 10.6 ppm; P$_i$: −0.071 ppm) (%) vs. exposition time (h)).

The residual PMG quantities were calculated from the corresponding ^{31}P NMR spectra using Equation (1):

$$PMG = \frac{S_{(PMG)}}{S_{(PMG)} + S_{(R-P)} + S_{(Pi)}} \times 100\%, \tag{1}$$

where $S_{(PMG)}$, $S_{(R-P)}$, and $S_{(Pi)}$ are the ^{31}P signals corresponding to PMG, phosphonic acids, and inorganic phosphate, respectively.

The ^{31}P NMR spectra of the degradation mixtures of PMG-H_2O_2-(UV) (UV; 25 °C) recorded for reactions carried out at pH = 2, 8, 10, and 12 are presented in Figure 11. For the identification of the reaction products of PMG-H_2O_2-(UV) mixtures, we recorded the ^{31}P NMR spectra of PMG potential degradation products. The chemical shifts ($\delta(^{31}$P)) of these compounds are listed in Table 6.

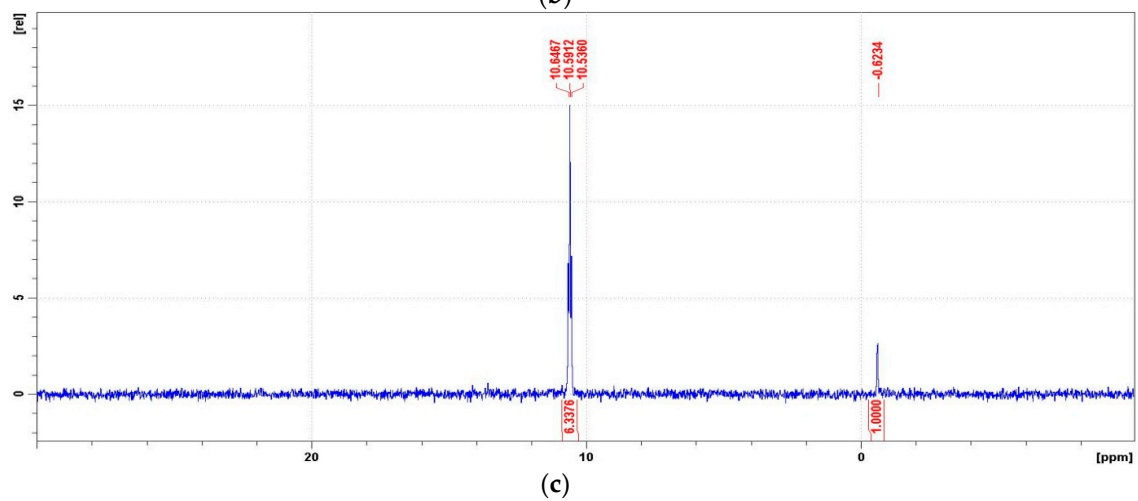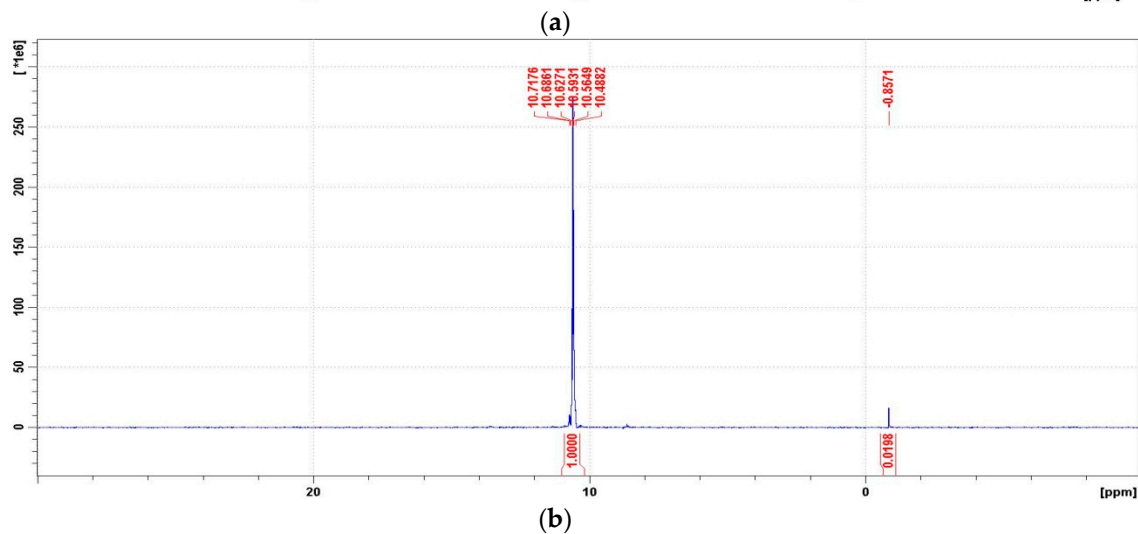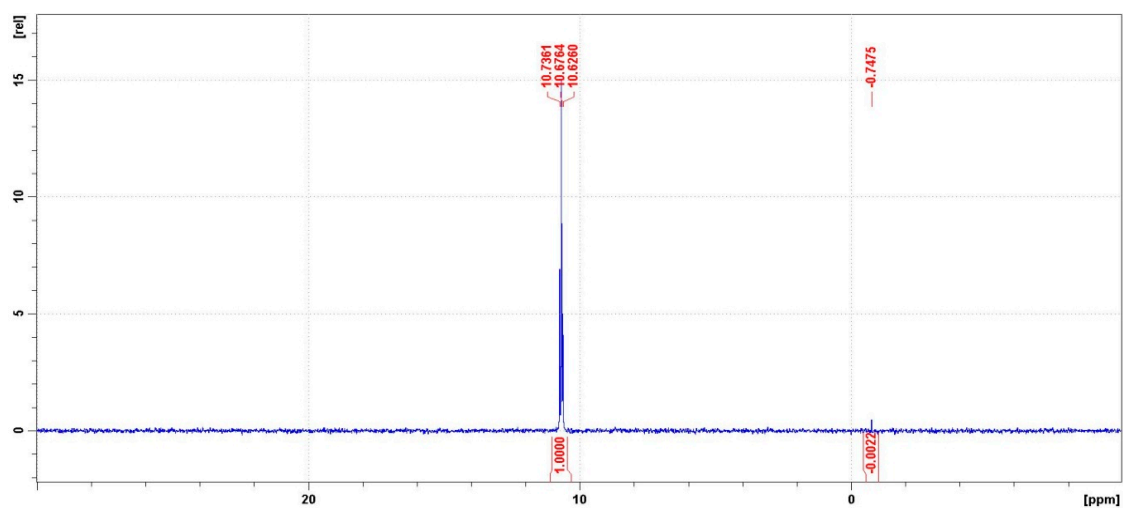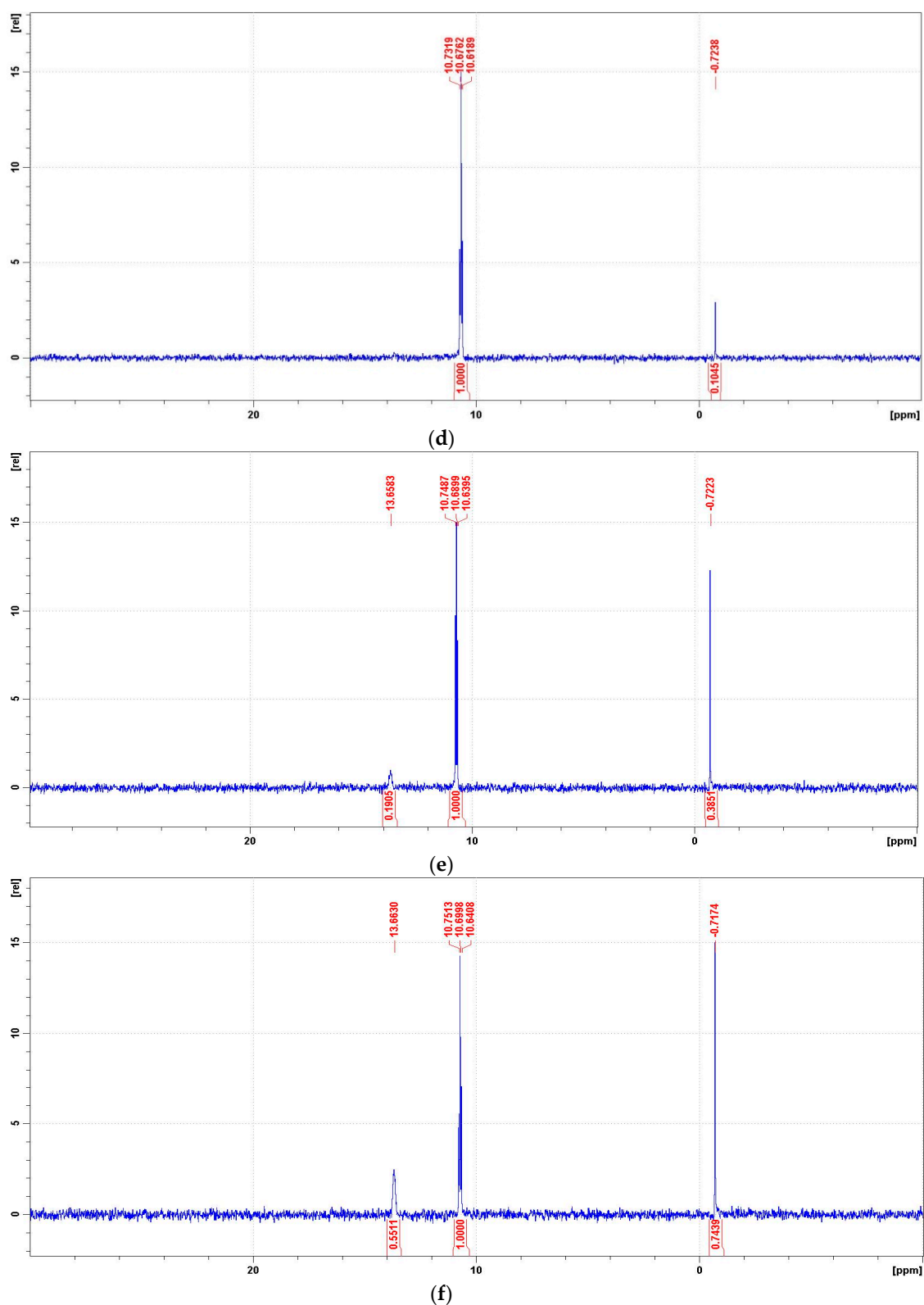**Figure 11.** *Cont.*

Figure 11. Representative ^{31}P NMR spectra of the degradation mixtures of PMG-H$_2$O$_2$-(UV) carried out at pH = 2–12 (UV; 25 °C), recorded after a given reaction time. (**a**) ^{31}P NMR spectrum of the reaction mixture recorded before radiation (dissolved in 2 M H$_2$SO$_4$/D$_2$SO$_4$/); (**b**) reaction mixture after UV radiation at pH = 2 (reaction time 360 min); (**c**) reaction mixture after UV radiation at pH = 8 (reaction time 360 min); (**d**) reaction mixture after UV radiation at pH = 10 (reaction time 360 min); (**e**) reaction mixture after UV radiation at pH = 12 (reaction time 30 min); (**f**) reaction mixture after UV radiation at pH = 12 (reaction time 360 min).

Table 6. ^{31}P Chemical shifts (δ(ppm)) of PMG and its potential degradation products in acidic and basic solutions.

2 M HCl							
Comp.	PMG	Gly^P	Me-Gly^P	Me$_2$-Gly^P	Me-PO$_3$H$_2$	H$_3$PO$_4$	H$_3$PO$_3$
δ (^{31}P) (ppm)	10.6	13.9	11.4	9.4	30.7	−0.47	5.15
2 M KOH							
Comp.	PMG	Gly^P	Me-Gly^P	Me$_2$-Gly^P	Me-PO$_3$H$_2$	H$_3$PO$_4$	H$_3$PO$_3$
δ (^{31}P) (ppm)	16.3	19.3	16.0	15.0	20.5	5.4	3.2

^{31}P δ(ppm): in 2 M HCl solutions (protonated forms of P-acids); in 2 M KOH solutions (deionized forms of P-acids).

The results of ^{31}P NMR investigations on PMG degradation with H$_2$O$_2$ are shown graphically in Figure 12.
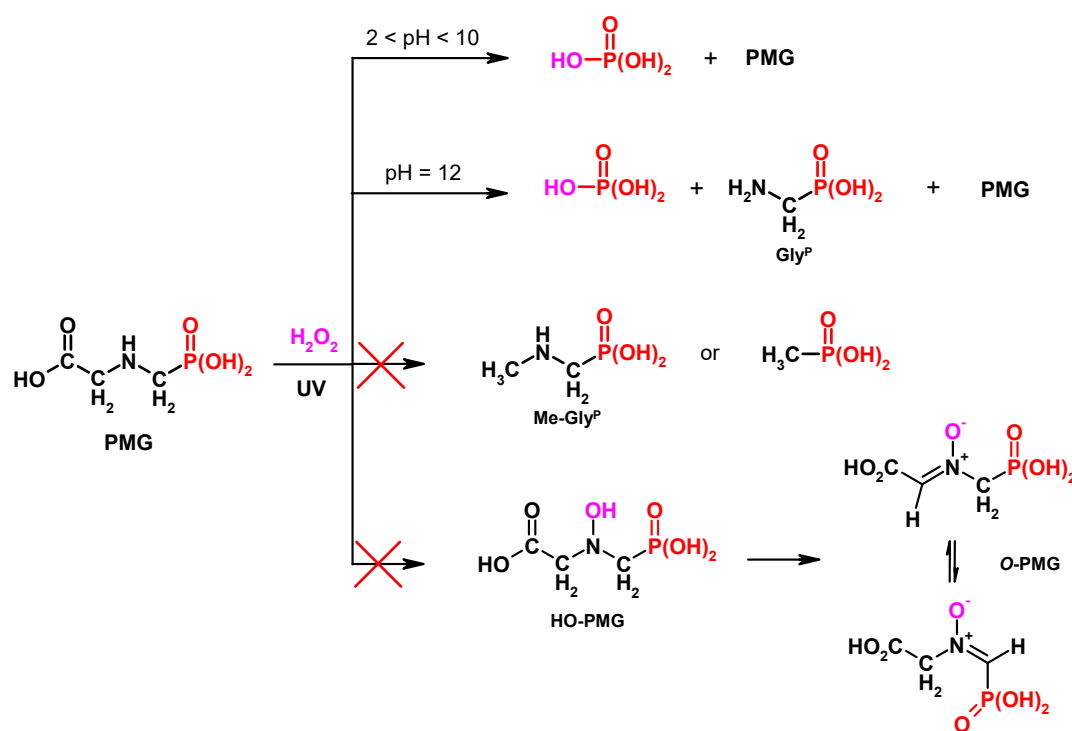
Figure 12. Possible degradation paths of PMG (reaction time: 48 h).

4. Conclusions

The data presented suggest the PMG inertness toward H$_2$O$_2$ in the modes without UV irradiation, both with (PMG-H$_2$O$_2$-Fe^{2+}) as well as without Fe^{2+} catalyst (PMG-H$_2$O$_2$). The data considering the reaction modes of PMG with H$_2$O$_2$ under UV irradiation (PMG- H$_2$O$_2$-(UV)) exhibit the slow degradation of PMG at $2 \leq$ pH ≤ 10, which becomes faster at pH = 12. The analysis of the ^{31}P NMR spectra of PMG-H$_2$O$_2$ reaction mixtures obtained for reactions carried out at $2 \leq$ pH ≤ 10 indicate the presence of initial PMG and H$_3$PO$_4$, and the mixture of PMG, Gly^P, and H$_3$PO$_4$/H$_x$PO$_4{}^{3-x}$ for reactions carried out at pH = 12. The results suggest the slow formation of an intermediate PMG × H$_2$O$_2$ phase in the first stage of degradation which decomposes very fast (no intermediates were observed in the ^{31}P NMR spectra) by the scission of the P-C bond of PMG and the subsequent release of phosphoric acid/phosphate ion.

Recapitulating, in the experiments carried out without UV radiation we observed:

- full stability of PMG in reaction with H_2O_2 (48 h);
- full stability of PMG in reaction with H_2O_2/Fe^{2+} (48 h).

In the experiments carried out with UV radiation (PMG-H_2O_2-(UV)), the P-C rapture type of PMG degradation was observed, the extent of which was dependent on the applied pH of the reaction mixtures. As a result, for the reactions run at $2 \leq \text{pH} \leq 10$, the partial formation of phosphoric acid/phosphate ions (PMG $\rightarrow$ PMG + $H_3PO_4/H_xPO_4^{3-x}$) was observed, whereas for reactions run at pH = 12, mixtures of PMG, Gly^P, and PO_4^{3-} were found.

We did not observe:

- any formation of nitrone-type derivatives (see [56–60]);
- the formation of Me-Gly^P (Sar^P) or Me-P(O)(OH)$_2$.

References

1. Franz, J.E.; Mao, M.K.; Sikorski, J.A. *Glyphosate: A Unique Global Herbicide*; American Chemical Society: Washington, DC, USA, 1997; ISBN 0841234582.
2. Dill, G.M.; Sammons, R.D.; Feng, P.C.C.; Kohn, F.; Kretzmer, K.; Mehrsheikh, A.; Bleeke, M.; Honegger, J.L.; Farmer, D.; Wright, D.; et al. Glyphosate: discovery, development, applications, and properties. In *Glyphosate Resistance in Crops and Weeds. History, Development and Management*; Nandula, V.K., Ed.; John Wiley & Sons, Inc.: Hoboken, NJ, USA, 2010; ISBN 978-0-470-41031-8.
3. Amrhein, N.; Deus, B.; Gehrke, P.; Steinrucken, H.C. The site of the inhibition of the shikimate pathway by glyphosate. II. Interference of glyphosate with chorismate formation in vivo and in vitro. *Plant Physiol.* **1980**, *66*, 830–834. [CrossRef] [PubMed]
4. Sikorski, J.A.; Gruys, K.J. Understanding glyphosate's molecular mode of action with EPSP synthase: Evidence favoring an allosteric inhibitor model. *Acc. Chem. Res.* **1997**, *30*, 2–8. [CrossRef]
5. Sviridov, A.V.; Shushkova, T.V.; Ermakova, I.T.; Ivanova, E.V.; Leontievsky, A.A. Glyphosate: Safety Risks, Biodegradation, and Bioremediation. In *Current Environmental Issues and Challenges*; Cao, G., Orru, R., Eds.; Springer Science+Business Media: Dordrecht, The Netherlands, 2014; pp. 183–195. [CrossRef]
6. Rampazzo, N.; Todorovic, G.; Mentler, A.; Blum, W.E.H. Adsorption of glyphosate and aminomethylphosphonic acid in soils. *Int. Agrophys.* **2013**, *27*, 203–209. [CrossRef]
7. Borggaard, O.K.; Gimsing, A.L. Fate of glyphosate in soil and the possibility of leaching to ground and surface waters: A review. *Pest. Manag. Sci.* **2008**, *64*, 441–456. [CrossRef]
8. Aparicio, V.C.; De Gerónimo, E.; Marino, D.; Primost, J.; Carriquiriborde, P.; Costa, J.L. Environmental fate of glyphosate and aminomethylphosphonic acid in surface waters and soil of agricultural basins. *Chemosphere* **2013**, *93*, 1866–1873. [CrossRef] [PubMed]
9. Mamy, L.; Barriuso, E.; Gabrielle, B. Glyphosate fate in soils when arriving in plant residues. *Chemosphere* **2016**, *154*, 425–433. [CrossRef] [PubMed]
10. Williams, G.M.; Kroes, R.; Munro, I.C. Safety evaluation and risk assessment of the herbicide Roundup and its active ingredient, glyphosate, for humans. *Regul. Toxicol. Pharmacol.* **2000**, *31*, 117–165. [CrossRef]
11. Mesnage, R.; Defarge, N.; Vendomois, J.S.; Seralini, G.E. Potential toxic effects of glyphosate and its commercial formulations below regulatory limits. *Food Chem. Toxicol.* **2015**, *84*, 133–153. [CrossRef]
12. Myers, J.P.; Antoniou, M.N.; Blumberg, B.; Caroll, L.; Colborn, T.; Everett, L.G.; Hansen, M.; Landrigan, P.J.; Lanphear, B.P.; Mesnage, R.; et al. Concerns over use of glyphosate-based herbicides and risks associated with exposures: A consensus statement. *Environ. Health* **2016**, *15*, 19. [CrossRef]

13. Guyton, K.Z.; Loomis, D.; Grosse, Y.; Ghissassi, F.; Benbrahim-Tallaa, L.; Guha, N.; Scoccianti, C.; Mattock, H.; Straif, K. Carcinogenicity of tetrachlorvinphos, parathion, malathion, diazinon, and glyphosate. *Lancet Oncol.* **2015**, *16*, 490–491. [CrossRef]

14. Anifandis, G.; Katsanaki, K.; Lagodonti, G.; Messini, C.; Simopoulou, M.; Dafopoulos, K.; Daponte, A. The effect of glyphosate on human sperm motility and sperm DNA fragmentation. *Int. J. Environ. Res. Public Health* **2018**, *15*, 1117. [CrossRef] [PubMed]

15. Anifandis, G.; Amiridis, G.; Dafopoulos, K.; Daponte, A.; Dovolou, E.; Gavriil, E.; Gorgogietas, V.; Kachpani, E.; Mamuris, Z.; Messini, C.I.; et al. The in vitro impact of the herbicide roundup on human sperm motility and sperm mitochondria. *Toxics* **2018**, *6*, 2. [CrossRef] [PubMed]

16. Rueppel, M.L.; Brightwell, B.B.; Schaefer, R.; Marvel, J.T. Metabolism and degradation of glyphosate in soil and water. *J. Agric. Food Chem.* **1977**, *25*, 517–528. [CrossRef] [PubMed]

17. Gohre, K.; Casida, J.E.; Ruzo, L.O. *N*-oxidation and cleavage of the amino acid derived herbicide glyphosate. *J. Agric. Food Chem.* **1987**, *35*, 388–392. [CrossRef]

18. Ikehata, H.; Gama El-Din, M. Aqueous pesticide degradation by hydrogen peroxide/ultraviolet irradiation and Fenton-type advanced oxidation processes: A review. *J. Environ. Eng. Sci.* **2006**, *5*, 81–135. [CrossRef]

19. Jaisi, D.P.; Li, H.; Wallace, A.F.; Paudel, P.; Sun, M.; Balakrishna, A.; Lerch, R.N. Mechanisms of bond cleavage during manganese oxide and UV degradation of glyphosate: Results from phosphate oxygen isotopes and molecular simulations. *J. Agric. Food Chem.* **2016**, *64*, 8474–8482. [CrossRef] [PubMed]

20. Barrett, K.A.; McBride, M.B. Oxidative degradation of glyphosate and amino-methylphosphonate by manganese oxide. *Environ. Sci. Technol.* **2005**, *39*, 9223–9228. [CrossRef] [PubMed]

21. Chen, Y.; Wu, F.; Lin, Y.; Deng, N.; Bazhin, N.; Glebov, E. Photodegradation of glyphosate in the ferrioxalate system. *J. Hazard. Mater.* **2007**, *148*, 360–365. [CrossRef]

22. Muneer, M.; Boxall, C. Photocatalyzed degradation of a pesticide derivative glyphosate in aqueous suspensions of titanium dioxide. *Int. J. Photoenergy* **2008**. [CrossRef]

23. Echavia, G.R.M.; Matzusawa, F.; Negishi, N. Photocatalytic degradation of organophosphate and phosphonoglycine pesticides using TiO_2 immobilized on silica gel. *Chemosphere* **2009**, *76*, 595–600. [CrossRef]

24. Assalin, M.R.; De Moraes, S.G.; Queiroz, S.C.; Ferracini, V.; Duran, N. Studies on degradation of glyphosate by several oxidative chemical processes: ozonation, photolysis and heterogeneous photocatalysis. *J. Environ. Sci. & Health B* **2010**, *45*, 89–94. [CrossRef]

25. Manassero, A.; Passalia, C.; Negro, A.C.; Cassano, A.; Zalazar, C.S. Glyphosate degradation in water employing the H_2O_2/UV-C process. *Water Res.* **2010**, *44*, 3875–3882. [CrossRef]

26. Paudel, P.; Negusse, A.; Jaisi, D.P. Birnessite-catalyzed degradation of glyphosate: a mechanistic study aided by kinetics batch studies and NMR spectroscopy. *Soil Sci. Soc. Am. J.* **2015**, *79*, 815–825. [CrossRef]

27. Kudzin, Z.H.; Gralak, D.K.; Drabowicz, J.; Łuczak, J. Novel approach for the simultaneous analysis of glyphosate and its metabolites. *J. Chromatogr. A* **2002**, *947*, 129–141. [CrossRef]

28. Kudzin, Z.H.; Gralak, D.K.; Andrijewski, G.; Drabowicz, J.; Łuczak, J. Simultaneous analysis of biologically active aminoalkanephosphonic acids. *J. Chromatogr. A* **2003**, *998*, 183–199. [CrossRef]

29. Cartigny, B.; Azaroual, N.; Imbenotte, M.; Mathieu, D.; Vermeersch, G.; Goulle, J.P.; Lhermitte, M. Determination of glyphosate in biological fluids by ^{1}H and ^{31}P NMR spectroscopy. *Forensic. Sci. Int.* **2004**, *143*, 141–145. [CrossRef] [PubMed]

30. Lipok, J.; Wieczorek, D.; Jewginski, M.; Kafarski, P. Prospects of in vivo ^{31}P NMR method in glyphosate degradation studies in whole cell system. *Enzyme Microb. Technol.* **2009**, *44*, 11–16. [CrossRef]

31. Ge, X.; d'Avignon, D.A.; Ackerman, J.J.H.; Sa, R.D. In vivo ^{31}P-Nuclear Magnetic Resonance studies of glyphosate uptake, vacuolar sequestration, and tonoplast pump activity in glyphosate-resistant horseweed. *Plant Physiol.* **2014**, *166*, 1256–1268. [CrossRef]

32. Cai, H.; Chuang, W.G.; Cui, X.; Cheng, R.H.; Chiu, K.; Chen, Z.; Ding, S. High Resolution ^{31}P NMR Spectroscopy generates a quantitative evolution profile of phosphorous translocation in germinating sesame seed. *Sci. Rep.* **2018**, *8*, 359. [CrossRef]

33. Kudzin, M.H.; Drabowicz, J.; Jordan, F.; Kudzin, Z.H.; Urbaniak, P. Reactivity of aminophosphonic acids. 3. Reaction with hydrogen peroxide. *Phosphorus Sulfur Silicon Relat. Elem.* **2018**, *193*. in press. [CrossRef]

34. Soroka, M. Comments on the synthesis of aminomethylphosphonic acid. *Synthesis* **1989**, 547–548. [CrossRef]

35. Hellmann, H. New methods of organic preparative chemistry. 8. Amidomethylation. *Angew. Chem.* **1957**, *69*, 463–471. [CrossRef]

36. Maier, L. Organic phosphorus compounds. Part 98. Synthesis of *N*-methylaminomethylphosphonic acid and derivatives. *Phosphorus Sulfur Silicon Relat. Elem.* **1991**, *62*, 29–34. [CrossRef]

37. Fields, E.K. The Synthesis of esters of substituted amino phosphonic acids. *J. Am. Chem. Soc.* **1952**, *74*, 1527–1531. [CrossRef]

38. Kudzin, Z.H.; Kudzin, M.H.; Drabowicz, J.; Stevens, C. Aminophosphonic acids—Phosphorus analogues of natural amino acids. Part 1: Syntheses of α-aminophosphonic acids. *Curr. Org. Chem.* **2011**, *15*, 2015–2071. [CrossRef]

39. Drabowicz, J.; Jakubowski, H.; Kudzin, M.H.; Kudzin, Z.H. The nomenclature of 1-aminoalkylphosphonic acids and derivatives: Evolution of the code system. *Acta Biochim. Pol.* **2015**, *62*, 139–150. [CrossRef]

40. Sprankle, P.; Meggitt, W.F.; Penner, D. Adsorption, mobility, and microbial degradation of glyphosate in the soil. *Weed Sci.* **1975**, *23*, 224–234. [CrossRef]

41. Wauchope, D. Acid Dissociation constants of arsenic acid, methylarsonic acid (MAA), dimethylarsinic acid (cacodylic acid), and *N*-(Phosphonomethyl)glycine (Glyphosate). *J. Agric. Food Chem.* **1976**, *24*, 717–721. [CrossRef]

42. Appleton, T.; Hall, J.; McMahon, I. NMR spectra of iminobis(methylenephosphonic acid), $HN(CH_2PO_3H_2)_2$, and related ligands and of their complexes with platinum(II). *Inorg. Chem.* **1986**, *25*, 726–734. [CrossRef]

43. Castellino, S.; Leo, G.; Sammons, R.D.; Sikorski, J. ^{31}P, ^{15}N, and ^{13}C NMR of glyphosate: Comparison of pH titrations to the herbicidal dead-end complex with 5-enolpyruvoylshikimate-3-phosphate synthase. *Biochemistry* **1989**, *28*, 3856–3868. [CrossRef]

44. Barja, B.C.; Dos Santos Afonso, M. An ATR−FTIR study of glyphosate and its Fe(III) complex in aqueous solution. *Environ. Sci. Technol.* **1998**, *32*, 3331–3335. [CrossRef]

45. Peixoto, M.M.; Bauerfeldt, G.F.; Herbst, M.H.; Pereira, M.S.; Da Silva, C.O. Study of the stepwise deprotonation reactions of glyphosate and the corresponding pK_a values in aqueous solution. *J. Phys. Chem. A* **2015**, *119*, 5241–5249. [CrossRef] [PubMed]

46. Liu, B.; Dong, L.; Yu, Q.; Li, X.; Wu, F.; Tan, Z.; Luo, S. Thermodynamic study on the protonation reactions of glyphosate in aqueous solution: potentiometry, calorimetry and NMR spectroscopy. *J. Phys. Chem. B* **2016**, *120*, 2132–2137. [CrossRef] [PubMed]

47. Alderighi, L.; Gans, P.; Ienco, A.; Peters, D.; Sabatini, A.; Vacca, A. Hyperquad simulation and speciation (HySS): a utility program for the investigation of equilibria involving soluble and partially soluble species. *Coord. Chem. Rev.* **1999**, *184*, 311–318. [CrossRef]

48. Ermakov, A.N.; Larin, I.K.; Kozlov, Y.N.; Purmal, A.P. The thermodynamic characteristics of hydrogen peroxide in H_2SO_4-H_2O solutions. *Russ. J. Phys. Chem.* **2006**, *80*, 1895–1901. [CrossRef]

49. Kwon, B.G.; Lee, J.H. Determination of hydroperoxyl/superoxide anion radical (HO_2/O_2^-) concentration in the decomposition of ozone using a kinetic method. *Bull. Korean Chem. Soc.* **2006**, *27*, 1785–1800. [CrossRef]

50. Mierzwa, J.C.; Rodrigues, R.; Teixeira, A.C.S.C. UV-Hydrogen Peroxide Processes. In *Advanced Oxidation Processes for Wastewater Treatment: Emerging Green Chemical Technology*; Chpt. 2; Elsevier Inc.: Amsterdam, The Netherlands, 2018; pp. 13–48.

51. Aust, S.D.; Morehouse, L.A.; Thomas, C.E. Role of metals in oxygen radical reactions. *J. Free Radic. Biol. Med.* **1985**, *1*, 3–25. [CrossRef]

52. Haber, F.; Weiss, J. The catalytic decomposition of hydrogen peroxide by iron salts. *Proc. R. Soc. Lond. Ser. A* **1934**, *147*, 332–335. [CrossRef]

53. Weinstein, J.; Bielski, B.H.J. Kinetics of the interaction of HO_2 and O_2 radicals with hydrogen peroxide. The Haber-Weiss reaction. *J. Am. Chem. Soc.* **1979**, *101*, 58–62. [CrossRef]

54. Zepp, R.G.; Faust, B.C.; Hoigne, J. Hydroxyl radical formation in aqueous reactions (pH 3-8) of iron(II) with hydrogen peroxide: The Photo-Fenton Reaction. *Environ. Sci. Technol.* **1992**, *26*, 313–319. [CrossRef]

55. Duesterberg, C.K.; Mylon, S.E.; Waite, T.D. pH effects on iron-catalyzed oxidation using Fenton's Reagent. *Environ. Sci. Technol.* **2008**, *42*, 8522–8527. [CrossRef] [PubMed]

56. Rawalay, S.S.; Shechter, H. Oxidation of primary, secondary, and tertiary amines with neutral permanganate. Simple method for degrading amines to aldehydes and ketones. *J. Org. Chem.* **1967**, *32*, 3129–3131. [CrossRef]

57. Mitsui, H.; Zenki, S.I.; Shiota, T.; Murahashi, S.I. Tungstate catalyzed oxidation of secondary amines with hydrogen peroxide. A novel transformation of secondary amines into nitrones. *J. Chem. Soc. Chem. Commun.* **1984**, 874–875. [CrossRef]

58. Kudzin, Z.H.; Drabowicz, J.; Skowroński, R. Synthesis of alkanephosphonates containing nitrone moiety. *Phosphorus Sulfur Silicon Relat. Elem.* **1990**, *51*, 310. [CrossRef]

59. Murahashi, S.I.; Mitsui, H.; Shiota, T.; Tsuda, T.; Watanabe, S. Tungstate-catalyzed oxidation of secondary amines to nitrones. α-Substitution of secondary amines via nitrones. *J. Org. Chem.* **1990**, *55*, 1736–1744. [CrossRef]

60. Colladon, M.; Scarso, A.; Strukul, G. Mild catalytic oxidation of secondary and tertiary amines to nitrones and *N*-oxides with H$_2$O$_2$ mediated by Pt(II) catalysts. *Green Chem.* **2008**, *10*, 793–798. [CrossRef]